

General Disclaimer

One or more of the Following Statements may affect this Document

- This document has been reproduced from the best copy furnished by the organizational source. It is being released in the interest of making available as much information as possible.
- This document may contain data, which exceeds the sheet parameters. It was furnished in this condition by the organizational source and is the best copy available.
- This document may contain tone-on-tone or color graphs, charts and/or pictures, which have been reproduced in black and white.
- This document is paginated as submitted by the original source.
- Portions of this document are not fully legible due to the historical nature of some of the material. However, it is the best reproduction available from the original submission.

CR-135007

REPORT NO. LMSC/D386845

DATED 26 February 1974

(NASA-CR-135007) VAPOR INGESTION IN A
CYLINDRICAL TANK WITH A CONCAVE ELLIPTICAL
BOTTOM (Lockheed Missiles and Space Co.)
19 p HC A02/MF A01

N77-21248

CSCI 211

Unclass

G3/28 24427

LOCKHEED MISSILES & SPACE COMPANY

A GROUP DIVISION OF LOCKHEED AIRCRAFT CORPORATION
SUNNYVALE, CALIFORNIA

CR-135007

VAPOR INGESTION IN A CYLINDRICAL TANK
WITH A
CONCAVE ELLIPTICAL BOTTOM

By

Andrew Klavins

LOCKHEED MISSILES & SPACE COMPANY, INC.
1111 Lockheed Way, Sunnyvale, CA 94088

Prepared for
NASA-Lewis Research Center, Cleveland, OH 44135
Under Contract NAS 3-17798,
Numerical Simulation of Low-Gravity Draining

APR 1 1974
RECEIVED
NASA STI FACILITY
INDIT BRANCH

Approved: *[Signature]*
for J. W. Anderson, Manager
Spacecraft Thermodynamics
D/62-63

1. Report No. NASA CR-135007	2. Government Accession No.	3. Recipient's Catalog No.	
4. Title and Subtitle VAPOR INGESTION IN A CYLINDRICAL TANK WITH A CONCAVE ELLIPTICAL BOTTOM		5. Report Date	
		6. Performing Organization Code	
7. Author(s) Andrew Klavins		8. Performing Organization Report No. IMSC-D386845	
9. Performing Organization Name and Address Lockheed Missiles and Space Co., Inc. Space Systems Division Sunnyvale, CA 94088		10. Work Unit No.	
		11. Contract or Grant No. NAS3-17798	
12. Sponsoring Agency Name and Address National Aeronautics and Space Administration Washington, D.C. 20546		13. Type of Report and Period Covered Contractor Report	
		14. Sponsoring Agency Code	
15. Supplementary Notes Project Manager, E. P. Symons, Chemical Energy Division NASA Lewis Research Center, Cleveland, OH 44135			
16. Abstract An approximate analytical technique is presented for estimating the liquid residual in a tank of arbitrary geometry due to vapor ingestion at any drain rate and acceleration level. The bulk liquid depth at incipient pull-through is defined in terms of the Weber and Bond numbers and two functions that describe the fluid velocity field and free surface shape appropriate to the tank geometry. Numerical results are obtained for the Centaur LH ₂ tank using limiting approximations to these functions.			
17. Key Words (Suggested by Author(s)) Vapor Ingestion, Propellant Residual, Centaur LH ₂ Tank, Low-g Draining, Weber Number, Bond Number, Froude Number		18. Distribution Statement Unclassified-Unlimited	
19. Security Classif. (of this report) Unclassified	20. Security Classif. (of this page) Unclassified	21. No. of Pages 17	22. Price*

* For sale by the National Technical Information Service, Springfield, Virginia 22151

VAPOR INGESTION IN A CYLINDRICAL TANK
WITH A
CONCAVE ELLIPTICAL BOTTOM
by Andrew Klavins

INTRODUCTION

The objective of this study is to estimate the propellant residual in the Centaur vehicle. The propellant considered is liquid hydrogen; flow rates and acceleration levels of interest are summarized in Table I, and Figure 1 shows details of the tank geometry.

The residual estimates are based on the approximate analysis of Ref. 1, as extended to low - g conditions in Ref. 2. Due to the level of approximation involved in this analysis, the numerical results obtained must be interpreted with caution, and experimental support would be desirable.

In this study, the flow rate and acceleration level are represented by the Weber number W and Bond number B . The group $W/(1+B)$ is assumed to correlate vapor ingestion data at all W and B ; using the Bernoulli equation for a surface streamline, this group is expressed in terms of the liquid depth, the Bond number, and two functions that involve the fluid velocity field and surface shape. Plausibility arguments are used to approximate these functions in a manner appropriate to the Centaur geometry. These approximations are then used to generate numerical values of $W/(1+B)$ as a function of the bulk liquid depth and Bond number, and thus arrive at quantitative estimates of the propellant residual at the conditions of interest.

ANALYSIS

The essential features of the vapor ingestion analysis presented in Ref. 1 and modified to low-g conditions in Ref. 2 consist of (1) writing the Bernoulli equation for a surface streamline between a point immediately above the drain and a point far from the drain, (2) expressing the fluid velocity at the near point in terms of the flow rate, and the pressure drop along the streamline due to surface tension in terms of the surface curvature, and (3) applying a criterion

that defines incipient pull-through to relate the liquid depth at pull-through to flow rate and acceleration level. In this analysis, several approximate, limiting expressions are derived for the relations required in step 2.

Referring to Figure 2, the Bernoulli equation between a near point "0" and far point " ∞ " is

$$p_0 + \rho gh_0 + (1/2) \rho u_0^2 = p_\infty + \rho gh_\infty, \quad (1)$$

where p is the liquid pressure just below the surface, ρ is the liquid density, g the acceleration, directed as shown, h is the fluid surface height above a reference level, and u_0 is the fluid velocity immediately above the drain. The velocity at ∞ is assumed to be zero. Definition of a control area A serves to relate u_0 to the volumetric flow rate Q ,

$$u_0 A \equiv \int_A \vec{u} \cdot d\vec{A} = Q, \quad (2)$$

and the pressure difference $p_\infty - p_0$ is related to the surface curvature J ,

$$p_\infty - p_0 = -\sigma(J_\infty - J_0), \quad (3)$$

where σ is the surface tension. Substituting (2) and (3) into (1) and introducing the Bond number $B = \rho ga^2/\sigma$ and the Weber number $W = \rho Q^2/\pi^2 \sigma a^3$, where a is the tank radius, the Bernoulli equation becomes

$$\frac{W}{B} \frac{\pi^2 a^5}{2A^2} = h_\infty - h_0 - a^2(J_\infty - J_0)/B. \quad (4)$$

In Ref. 3, vapor ingestion data are correlated in terms of the Froude number $F = Q^2/ga^5$ at high g and the Weber number at zero g ; the analysis of Ref. 2 as well as current work at LMSC suggest that vapor ingestion data at all acceleration levels may be correlated in terms of the group $W/(1+B)$, which has the appropriate limiting values at $g \rightarrow 0, \infty$. Accordingly, (4) will be rewritten in terms of this parameter group.

It is the quantities A and $J_\infty - J_0$ that depend on the tank geometry and will be approximate in the present study; for convenience, the surface curvature term is replaced by the dimensionless function f defined as

$$f = - \frac{h_\infty - h_0}{a^2(J_\infty - J_0)} \quad (5)$$

The Bernoulli equation then becomes

$$\frac{W}{1+B} = \frac{2}{\pi^2 a^5} \frac{A^2}{f} \frac{1+Bf}{1+B} (h_{\infty} - h_o); \quad (6)$$

this relation depends on the tank geometry only through the control area A and the surface curvature function f.

At incipient pull-through, h_o decreases much more rapidly than h_{∞} ; this criterion is introduced into the Bernoulli equation by differentiating with respect to h_o and setting $dh_{\infty}/dh_o = 0$ at $h_o = h_{oc}$, $h_{\infty} = h_{\infty c}$:

$$h_{\infty c} - h_{oc} = \left[\frac{2}{A} \frac{\partial A}{\partial h_o} - \frac{1}{1+Bf} \frac{1}{f} \frac{\partial f}{\partial h_o} \right]^{-1}_c \quad (7)$$

This equation relates h and h_o at incipient pull-through, denoted by the subscript c. Setting $h_{\infty} = h_{\infty c}$ and $h_o = h_{oc}$ in (6) and using (7) to eliminate one of these variables yields the relationship between $W/(1+B)$ and residual depth, with Bond number as a parameter.

The results obtained so far are applicable to any tank geometry, subject only to the assumptions of irrotational, inviscid, quasi-steady flow, that the fluid fills the drain end of the tank, and that vortexing is not present. The analysis is specialized to a particular tank geometry through the functions A and f.

The control area function A

The choice of this function depends on the quantity of propellant in the tank and on the tank geometry. Several choices come to mind for various fluid levels, as detailed in Figure 3.

If the fluid surface is far removed from the drain, the velocity potential is well approximated by that of a point sink, as discussed Ref. 2, and the appropriate control area is a spherical surface, centered near the drain. This situation is depicted in Figure 3a. In view of the approximate nature of the analysis, the complexity of an exact expression for this area is not justified. Rather, the approximations indicated in the figure are used. Taking the sphere

radius to be the dip height h_o , with b the semi-minor axis of the ellipsoid that form the tank bottom, $A(h_o)$ in this case is given by

$$A(h_o) = \pi h_o^2 \left[1 - 1/6(h_o/a) - 2/3 \sqrt{1 - (d/h_o)^2} \right], \quad (8)$$

where

$$d/h_o = \frac{\sqrt{1 + (h_o/b)^2 (a^2/b^2 - 1)} - 1}{(h_o/a) (a^2/b^2 - 1)}. \quad (9)$$

This result corresponds to the limit of h_{oo} much larger than drain size discussed in Ref. 2.

If the fluid level is low enough, the velocity field will be essentially circumferential, and the control area is planar, as shown in Figure 3b.

The corresponding control area is

$$A(h_o) = 2ah_o - ab \left[(h_o/b) \sqrt{1 - (h_o/b)^2} + \sin^{-1} (h_o/b) \right] \quad (10)$$

The surface curvature function f

The expression to be used for this function depends strongly on the acceleration level, as observed in Refs. 4 and 5. At large Bond numbers, one expects an essentially flat liquid surface, while at small Bond number and a small contact angle, the surface is highly curved. As in the computation of the control areas, simple plausible shapes are assumed, as illustrated in Figure 4.

Cases (a) and (b) refer to the situation $h_o/b > 1$, where the control area is given by Equations (8) and (9). With $B \rightarrow 0$, the liquid surface is highly curved, and an order of magnitude estimate gives

$$f = 1/2, \quad h_o/b > 1, \quad B \ll 1. \quad (11)$$

With $B \rightarrow \infty$, the interface is essentially flat, and

$$f = 1/4, \quad h_o/b > 1, \quad B \gg 1. \quad (12)$$

Cases (c) and (d) refer to the situation $h_o/b < 1$, corresponding to the control area of Equation (10). In the $B \rightarrow 0$ limit, the surface of the bulk liquid is still curved as in case (a) but in the dip region the surface is visualized as a section of torus, with radius $R_o \ll R_{\infty}$.

The expression for f in this case is

$$f(h_o) = 1/2 \left[1 - \sqrt{1 - (h_o/b)^2} \right]^2, \quad h_o/b < 1, \quad B \ll 1. \quad (13)$$

In the $B \rightarrow \infty$ limit of case (d), the liquid surface is a flat ring, depressed by the amount $h_{\infty} - h_o$ in the vicinity of the drain, and f is given by

$$f = \pi^2/8, \quad h_o/b < 1, \quad B \gg 1. \quad (14)$$

When these expressions are substituted into Equations (6) and (7), the value of $W/(1+B)$ above which pull-through will occur can be computed as a function of liquid depth. Such calculations are discussed below. It is emphasized that the numerical values are a coarse approximation at best, and empirical support is desirable, particularly in the vicinity of $h_{\infty}/b \approx 1$, where it is not clear whether the deep - or shallow - tank analysis is appropriate, and at low B , where a relationship between the fluid height at pull-through and residual volume must be assumed.

RESULTS

Figure 5 is a summary of the results of calculations carried out using the various control area and surface curvature functions assumed for limiting cases.* Each curve shows the fluid height at which vapor ingestion may be expected to occur for a given value of $W/(1+B)$. Alternately, the curves give the maximum value of $W/(1+B)$ allowable at a given fluid level if vapor ingestion is to be avoided. The volumes indicated in Figure 5 at several pull-through depths assume that the liquid surface is flat, as in the $B \rightarrow \infty$ limit.

Referring to Table 1, an estimate can be made of whether or not pull-through will occur at the flow rates and acceleration levels of interest. During the

* The computation sequence is summarized in Table II.

start-up transient, with no settling thrust, $W/(1+B)$ peaks at about 9.3; extrapolation yields a pull-through height $h_{\infty c}/b \approx 3.3$, a value well above that corresponding to an initial propellant mass of 1467 lb_m. If a settling thrust of 24 lb_f is used, the peak $W/(1+B)$ is reduced to 6.3×10^{-3} and the pull-through height is $h_{\infty c}/b \approx 1.1$. The corresponding number for a settling thrust of 100 lb_f is $h_{\infty c}/b \approx .83$. These values are obtained with the control area assumed spherical; the pull-through height for the 100 lb_f thrust case assuming a planar control area is $h_{\infty c}/b \approx 1.1$. This difference represents an uncertainty of a factor of two in the residual volume calculation in the neighborhood of $h_{\infty c}/b \approx 1$; the actual case is expected to be somewhere between the two. From a design viewpoint, however, there is no problem if the initial level is at $h_0/b \approx 1.56$ corresponding to a 27.4% propellant loading.

An additional observation concerns operation of the vehicle at the full thrust of 30,000 lb_f. As propellant is expended, the vehicle mass decreases and the acceleration increases, decreasing $W/(1+B)$. The propellant level also decreases, however, lowering the maximum value of $W/(1+B)$, and introducing the possibility of vapor ingestion at full thrust. Figure 6 shows the actual and maximum values of $W/(1+B)$ as a function of burn time for the full thrust case assuming an initial LH₂ volume of 350 ft³, a constant LH₂ flow rate of 1241 gal/min, and several oxidizer/fuel ratios. On the basis of these calculations, one does not expect to encounter vapor ingestion before the bulk liquid level drops below the top of the sump region.

REFERENCES

1. Lubin, B. T., and M. Hurwits, "Vapor Pull-Through at a Tank Drain With and Without Dielectrophoretic Baffling", Proceedings of the Conference on Long-Term Cryopropellant Storage in Space, Huntsville, Alabama, 1966.
2. "Orbital Refueling and Checkout Study", Vol. 3, Part 2, Report T1-51-67-21, LMSC (NASA CR-93237), 1968.
3. Abdalla, K. L., and S. G. Berenyi, "Vapor Ingestion Phenomena in Weightlessness", NASA TN D-5210, 1969.
4. Reynolds, W. C., and H. M. Satterlee, Liquid Propellant Behavior at Low and Zero-g", Ch. 11, Dynamic Behavior of Liquids in Moving Containers, H. N. Abramson, Ed., NASA SP-106, 1966.
5. Derdul, J. D., L. S. Grubb, and D. A. Petrash, "Experimental Investigation of Liquid Outflow from Cylindrical Tanks During Weightlessness", NASA TN D-3746, 1966.

TABLE I
SUMMARY OF FLOW CONDITIONS

Propellant: liquid hydrogen, $\sigma/p = 26.6 \text{ cm}^3/\text{sec}^2$

Initial vehicle weight $W_0 = 14,024 \text{ lb}_m$

Initial propellant loading = $27.4\% \approx 350 \text{ ft}^3$

Acceleration levels, based on W_0 :

Thrust $T = 24 \text{ lb}_f$	$B = 1.47 \times 10^3$	Settling
$T = 100 \text{ lb}_f$	$B = 6.13 \times 10^3$	Settling
$T = 30,000 \text{ lb}_f$	$B = 1.84 \times 10^6$	Main Engine

Flow rates:

Time sec.	Q $\text{ft}^3/\text{sec.}$	$W/(1+B)$			
		$T = 0$	$T = 24 \text{ lb}_f$	$T = 100 \text{ lb}_f$	$T = 30,000 \text{ lb}_f$
10	.214	3.96×10^{-2}	2.69×10^{-5}	6.46×10^{-6}	--
28	.927	7.43×10^{-1}	4.37×10^{-4}	1.21×10^{-4}	--
29.95	3.275	9.28	6.31×10^{-3}	1.51×10^{-3}	--
30.35	2.675	6.64	4.57×10^{-3}	1.08×10^{-3}	3.36×10^{-6}

TABLE II
COMPUTATION SEQUENCE

(i) Pick Bond number and choice of A and f.

(ii) Pick $N_0 = h_{oc}/b$

(iii) Evaluate $A(N_0)$ and $f(N_0)$

(iv) Evaluate the derivatives

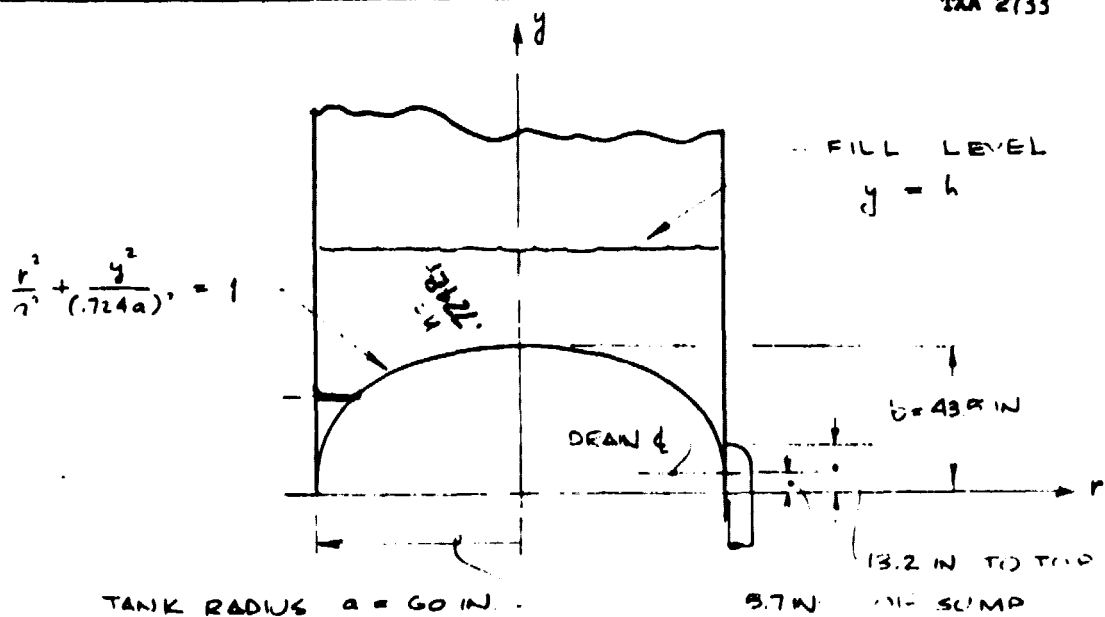
$$\frac{\partial A}{\partial h_0} \approx \frac{100}{b} \left[A(N_0 + .01) - A(N_0) \right],$$

$$\frac{\partial f}{\partial h_0} \approx \frac{100}{b} \left[f(N_0 + .01) - f(N_0) \right].$$

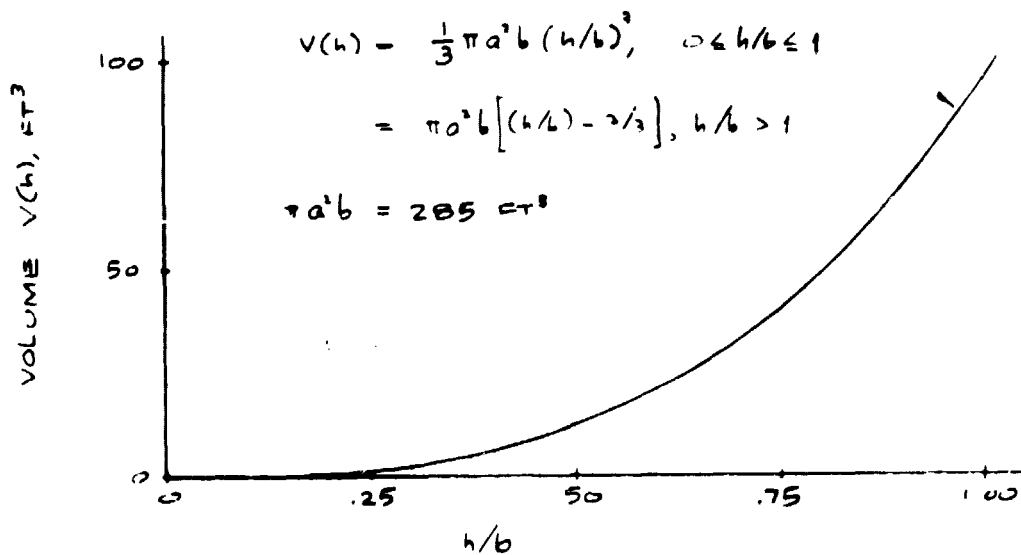
(v) Substitute the results of (iii) and (iv) into Eq. (7) to obtain $(h_{oc}/h_0)_c$

(vi) Substitute the results of (iii) and (v) into Eq. (6) to obtain $W/(1+B)$

Prepared by:	Date:	LOCKHEED MISSILES & SPACE COMPANY, INC.	Page 10
Checked by:	Date:	Title	Model
Approved by:	Date:		Report No. LMBC/D386845
			TXA 2733



(a) TANK BOTTOM CONFIGURATION



(b) VOLUME AS A FUNCTION OF LIQUID DEPTH ($b \gg 1$)

Prepared by:	Date	LOCKHEED MISSILES & SPACE COMPANY INC	Page 11
Checked by:	Date	Title	Model
Approved by:	Date		Report No. LMSC/DJ86845 REV 2733

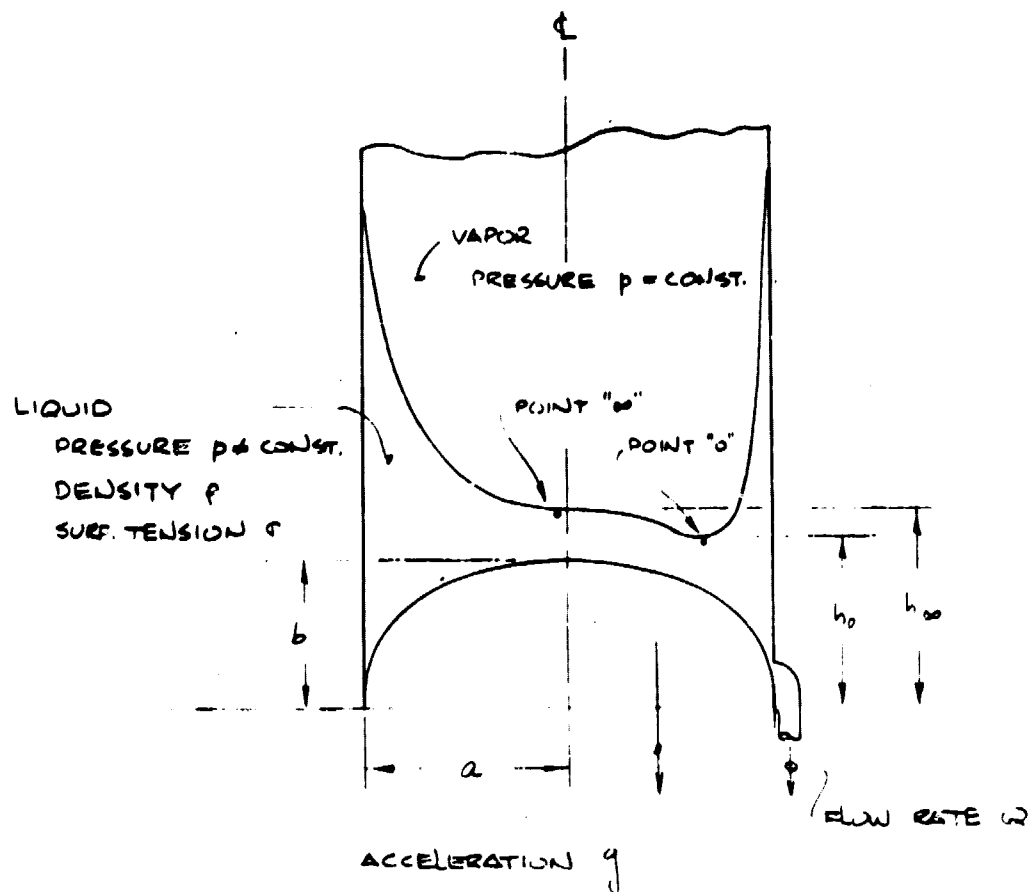
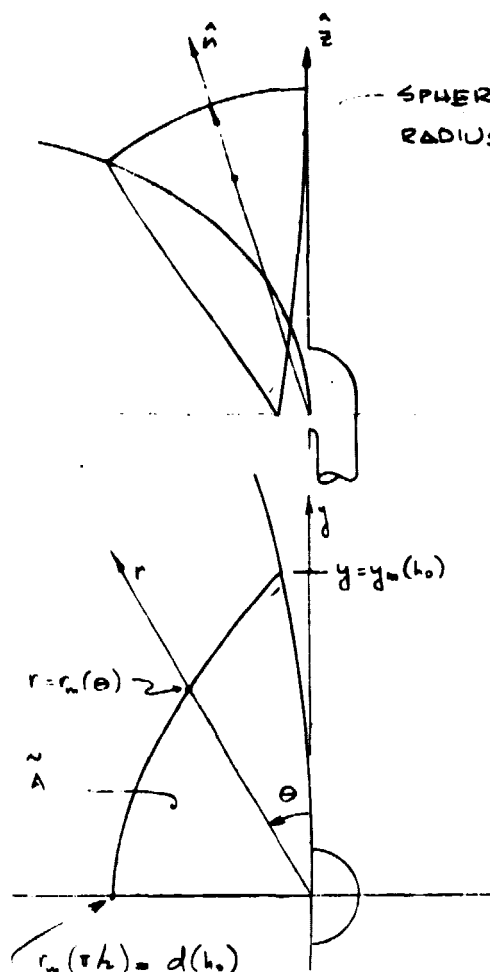


FIG. 2 LOW- g TANK DRAINING. DEFINITION
OF TERMS



$$A(h_0) = 2 \int \int_{\tilde{A}} \frac{r dr d\theta}{\hat{n} \cdot \hat{z}}$$

$$\hat{n} \cdot \hat{z} = \sqrt{1 - r^2/h_0^2}$$

$$d/h_0 = \frac{\sqrt{1 + (h_0/b)^2 (a^2/b^2 - 1)} - 1}{(h_0/a) \sqrt{a^2/b^2 - 1}}$$

$$y_h(h_0) = h_0 \sqrt{1 - (h_0/2a)^2}$$

$$\Rightarrow A(h_0) = 2h_0^2 \int_{\theta_{min}}^{\theta_h} [1 - \sqrt{1 - (r_h(\theta)/h_0)^2}] d\theta$$

$$\sqrt{1 - (r_h(\theta)/h_0)^2} \approx K_1 + K_2 \theta + K_3 \theta^2$$

$$K_1 = h_0/2a, K_2 = \frac{4}{\pi} [\sqrt{1 - (d/h_0)^2} - h_0/2a]$$

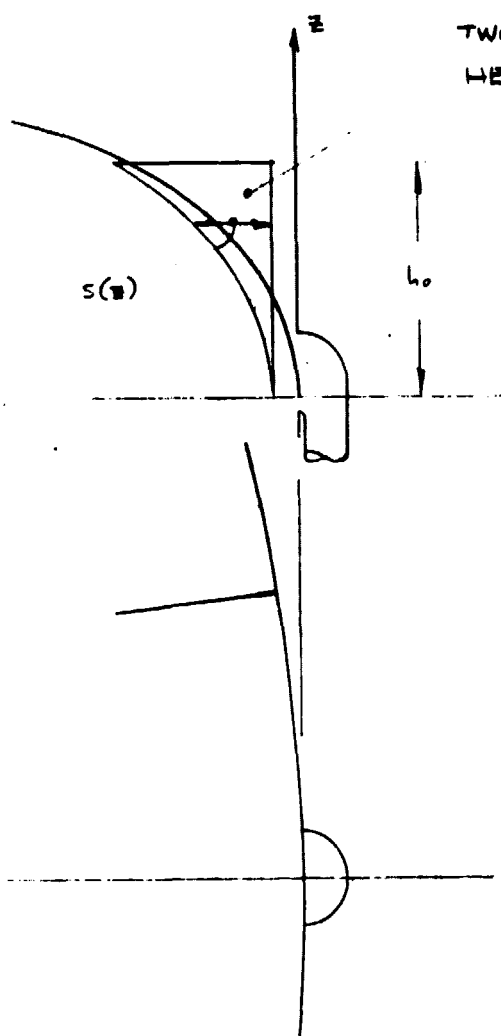
$$K_3 = -K_2/\pi$$

$$\Rightarrow A(h_0) \approx \pi h_0^2 \times$$

$$\times \left\{ 1 - \frac{1}{6} \frac{h_0^2}{a^2} - \frac{2}{3} \sqrt{1 - \left(\frac{d}{h_0}\right)^2} \right\}$$

FIG 3 APPROXIMATIONS TO CONTROL AREA FUNCTION.

(a) $h_0/b > 1$.



TWO PLANAR SURFACES
HEIGHT h_0

$$A(h_0) = 2 \int_0^{h_0} s(z) dz$$

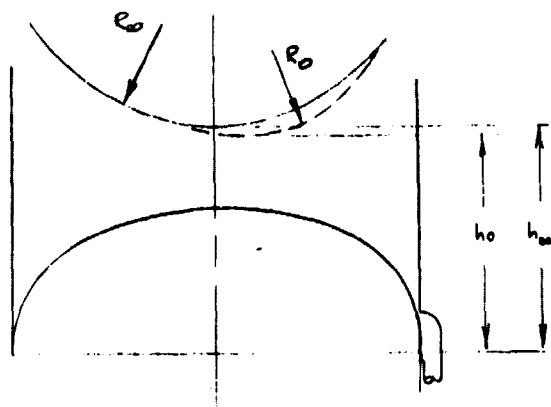
$$s(z) = a \left[1 - \sqrt{1 - (z/b)^2} \right]$$

$$A(h_0) = 2ab \times$$

$$\times \left\{ \frac{h_0}{b} - \frac{h_0}{2b} \sqrt{1 - \left(\frac{h_0}{b}\right)^2} - \frac{1}{2} \sin^{-1} \left(\frac{h_0}{b}\right) \right\}$$

FIG. 3 (CONT.) APPROXIMATIONS TO CONTROL AREA
FUNCTION. (b) $h_0/b < 1$.

UMSC/D386945
TXA 2733



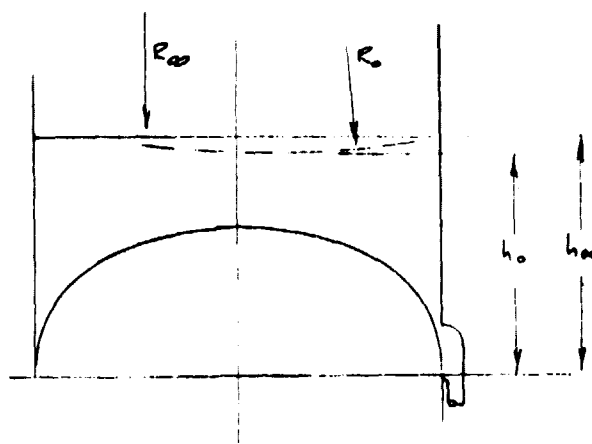
(a) $h_0/b > 1$, $B \ll 1$

$$R_\infty \approx a$$

$$R_0 \approx a - (h_\infty - h_0)$$

$$\begin{aligned} J_\infty - J_0 &= \frac{2}{R_\infty} - \frac{2}{R_0} \\ &\approx \frac{2}{a} - \frac{2}{a - (h_\infty - h_0)} \\ &\approx -\frac{2(h_\infty - h_0)}{a^2} \end{aligned}$$

$$\begin{aligned} f &= -\frac{1}{a^2} \frac{h_\infty - h_0}{J_\infty - J_0} \\ &= \frac{1}{2} = \text{CONST.} \end{aligned}$$



(b) $h_0/b > 1$, $B \gg 1$

$$R_\infty = \infty$$

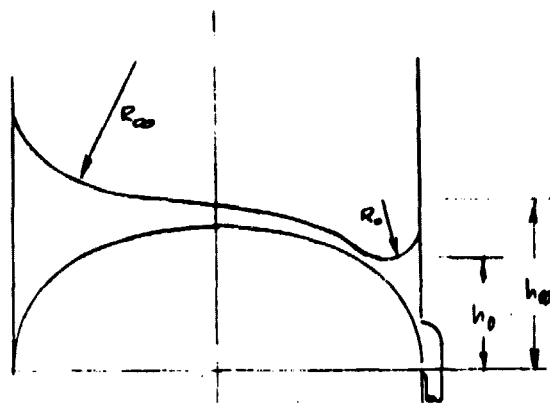
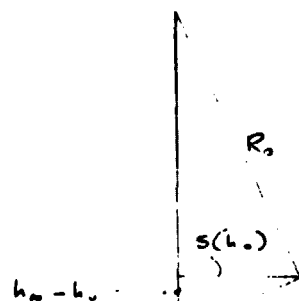
$$R_0 \approx \frac{a^2}{2(h_\infty - h_0)}$$

$$\begin{aligned} J_\infty - J_0 &= \frac{2}{R_\infty} - \frac{2}{R_0} \\ &\approx -\frac{4(h_\infty - h_0)}{a^2} \end{aligned}$$

$$f = \frac{1}{4} = \text{CONST.}$$

FIG. 4 APPROXIMATIONS TO SURFACE CURVATURE

FUNCTION. $h_0/b > 1$.

(c) $h_0/b < 1$, $B \ll 1$ 

$$s(h_0) = a \left[1 - \sqrt{1 - (h_0/b)^2} \right]$$

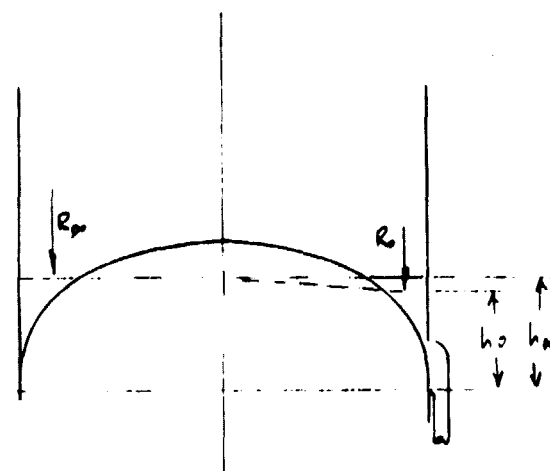
$$R_\infty = a$$

$$R_0 = \frac{s'(h_0)}{2(h_\infty - h_0)} \ll R_\infty$$

$$J_\infty - J_0 = \frac{2}{R_\infty} - \frac{1}{R_0}$$

$$\approx -\frac{2(h_\infty - h_0)}{s'(h_0)}$$

$$f(h_0) = \frac{s'(h_0)}{2a^2}$$

(d) $h_0/b < 1$, $B \gg 1$

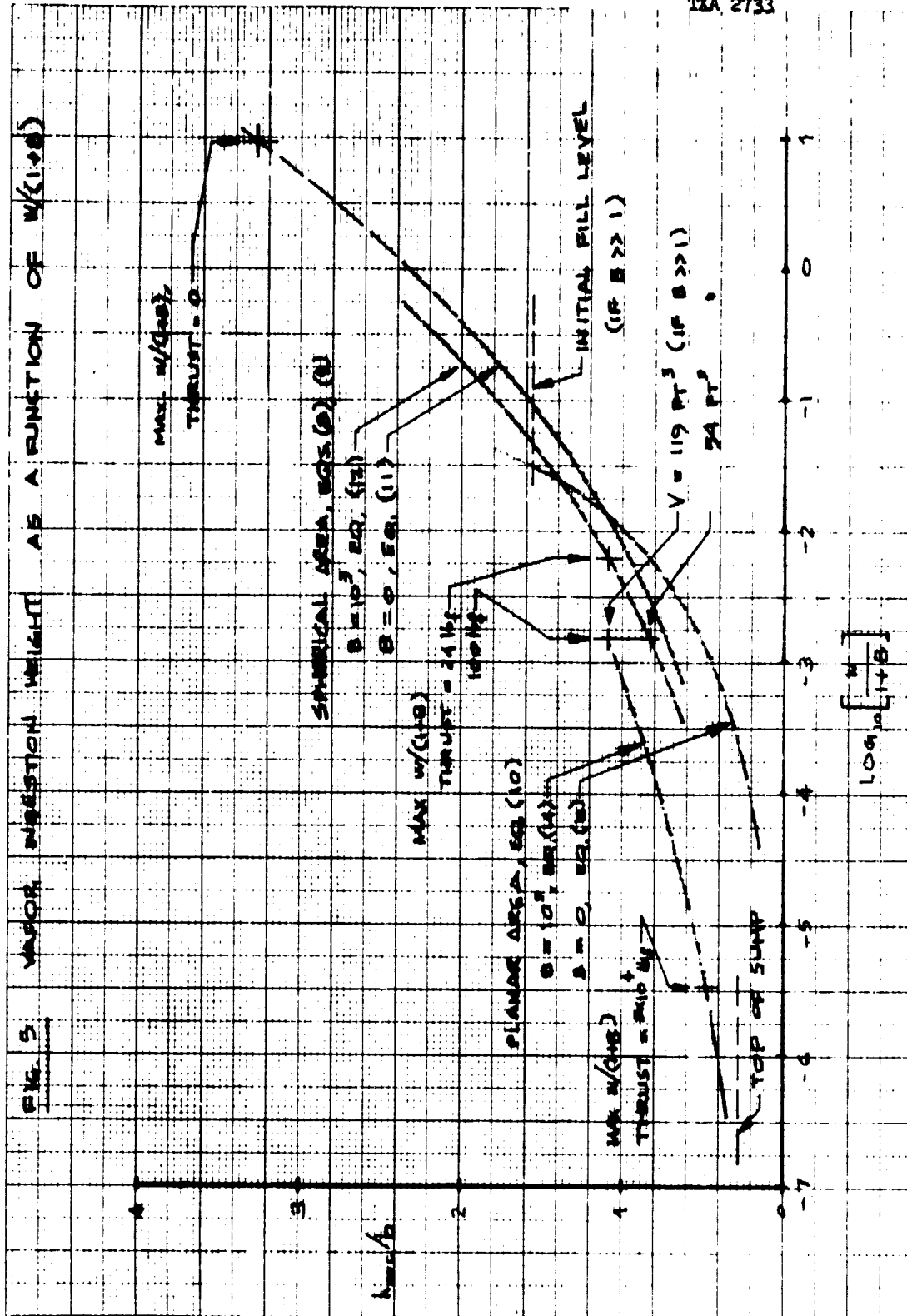
$$R_\infty = \infty$$

$$R_0 = \frac{(\pi a/2)^2}{2(h_\infty - h_0)}$$

$$J_\infty - J_0 = \frac{2}{R_\infty} - \frac{1}{R_0} \\ = \frac{\pi^2 a^2}{8(h_\infty - h_0)}$$

$$f = \frac{\pi^2}{8} = \text{CONST.}$$

FIG. 4 (CONT.). APPROXIMATIONS TO SURFACE CURVATURE
FUNCTION. $h_0/b < 1$.



IMSC/D386845
TXA 2733

FIG. 6 COMPARISON OF ACTUAL AND MAXIMUM
VALUE OF $W/(1+B)$ DURING FULL THROST
BURN. INITIAL FILL LEVEL = 250 GT³.

